

# Use of a partial local density of states calculation to characterize the Auger electron Si- $L_{2,3}$ $VV$ transitions of thin oxide layers

A. G. B. M. Sasse, H. Wormeester, M. A. van der Hoef, E. G. Keim, and A. van Silfhout  
University of Twente, Department of Applied Physics, P. O. Box 217, 7500 AE, Enschede, The Netherlands

(Received 2 September 1988; accepted 17 October 1988)

The line shape of the Si- $L_{2,3}$   $VV$  Auger spectrum is to a first approximation equal to the sum of the convolution products of the partial local density of states (pLDOS), each weighted by the two electron Auger matrix elements and the escape depth. Semiempirical quantum chemical cluster calculations have been used to calculate the pLDOS of  $\text{SiO}_x$  ( $x = 0, 0.5, 1, 1.5, 2$ ) from which the line shape in the derivative mode [ $dN(E)/dE$ ] could be obtained by using the angular momentum selection rules of Feibelman *et al.*, neglecting the structure in the radial two electron Auger matrix elements. Within this approximation we were able to interpret peaks in the measured Si- $L_{2,3}$   $VV$  Auger line shape of the initial oxidized silicon surfaces (100, 111, 110) and the fully oxidized Si(100) in the derivative mode in terms of local chemical bonding.

The development of complex integrated circuits in the semiconductor industry requires a detailed fundamental understanding of interfaces with device dimensions of several fundamental scaling lengths.<sup>1</sup> SiO layers play an important role as interface in electronic devices. Thin SiO layers, thermally grown, are in general composed of several chemical species of Si-O bonds (Si-Si<sub>n</sub>O<sub>4-n</sub>;  $n = 0, 1, \dots, 4$ ). Sample preparation, ultrahigh vacuum conditions, gas species, and oxidation temperature strongly determine the ratio of the several chemical compounds of SiO<sub>x</sub>.<sup>2</sup> Auger  $L_{2,3}$   $VV$  Auger electron spectroscopy is a surface sensitive probe and can therefore be used to study the SiO<sub>x</sub> interface.<sup>3-5</sup>

The aim of this paper is to illustrate that quantum chemical calculations compared with the Auger line shape in the derivative mode,  $dA(E)/dE$ , result in a powerful scheme for the interpretation of the Si- $L_{2,3}$   $VV$  Auger line shape in terms of atomic valence electron distributions. By simulating the  $dA(E)/dE$  of the Si- $L_{2,3}$   $VV$  Auger spectra using a calculated real-space partial local density of states (pLDOS), chemical and geometric information of the bonds involved in the silicon oxygen interface can be recognized straightforward from the measured loss corrected derivative Auger line shape,  $dA(E)/dE$ .

Within the independent particle approximation and due to the core-hole localization, Feibelman *et al.*<sup>7</sup> showed that the Auger line shape can be expressed in terms of angular momentum weighted atomic Auger matrix elements and of angular momentum components of the LDOS localized on the same site as the core-hole. If the line shape does not reflect the final-state hole configuration, which is the case for  $s$ - $p$  materials such as silicon,<sup>8-13</sup> information about the local density of occupied states can be obtained. Under this assumption we can express the Auger line shape in terms of convolution products of the pLDOS:

$$A(E) = C_{ss} N_s(E) * N_s(E) + C_{sp} N_s(E) * N_p(E) + C_{pp} N_p(E) * N_p(E), \quad (1)$$

where  $C_{kn}$  ( $n, k = s, p$ ) are the atomic Auger matrix elements and  $N_k(E)$  are the  $k$ -like LDOS at the atom in which the initial hole is produced.

The variation in the two electron Auger matrix elements  $C_{kn}$ , across the valence band, is predominantly due to the number of decaying channels for the Auger electrons ( $pp:46, sp:24, ss:3$ ),<sup>7</sup> which is governed by the selection rules of the angular momentum of the electrons involved in the Auger process.<sup>7-15</sup> By differentiating the calculated kinetic energy distribution  $A(E)$  we obtain the  $dA(E)/dE$  spectrum, which can be compared directly with the loss corrected differentiated experimental spectrum. The derivative mode is preferred since it exhibits more clearly the fine structure present. We can calculate the derivative applying our spline based numerical differentiation method.<sup>6</sup>

The linear combination of atomic orbitals-molecular orbitals (LCAO-MO) theory and the usefulness of its application to molecules is well known.<sup>16,17</sup>

Due to the extreme local behavior of the Si- $L_{2,3}$   $VV$  Auger process<sup>3</sup> it is possible to use a quantum chemical cluster scheme to calculate the local atomic electron distribution of the surface atoms as a function of the angular momentum of the valence electrons. For our calculations we have adapted the semiempirical quantum chemical method MINDO/3<sup>17,18</sup> and made it suitable for modeling half-infinite solid surfaces as is discussed extensively elsewhere.<sup>4</sup> One of the main advantages using this kind of calculation is that we reveal a real-space pLDOS. This gives us the ability to evaluate the influence of the several types of Si-surface atoms such as backbond atoms and dimer atoms [Si(100)] on the Auger line shape.

We have used a Si<sub>9</sub>O<sub>x</sub>H<sub>14</sub> ( $x = 2, 3, 4, 5$ ) cluster to model oxygen chemisorption on the Si(100)  $2 \times 1$  reconstructed surface (see Fig. 1). For the subsurface atoms the ideal bulk geometry of silicon ( $d_{\text{Si-Si}} = 2.35 \text{ \AA}$ , and tetrahedral angles) has been used, whereas the surface atoms are subject to an asymmetric  $2 \times 1$  reconstruction<sup>19,20</sup> as reported by Kunjunny and Ferry.<sup>15</sup>

To avoid the generation of fictitious surface states, which could interact with the real surface states, thus severely affecting the final results,<sup>21</sup> we used hydrogen atoms to terminate the silicon substrate and obtaining boundary conditions of sufficient quality. The value attributed to the Si-H bond

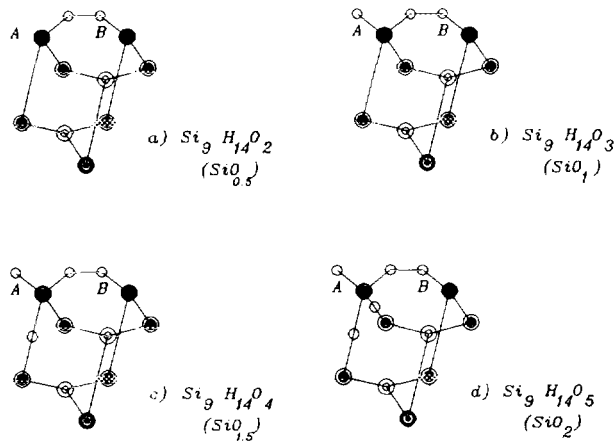


FIG. 1.  $\text{Si}_x\text{O}_x\text{H}_{14}$  cluster: (a)  $x = 2$ , (b)  $x = 3$ , (c)  $x = 4$ , and (d)  $x = 5$ . The LDOS is obtained at atom A. The dangling bonds at the first layer are not drawn. The other unsaturated silicon bonds are terminated by hydrogen atoms ( $d = 1.41 \text{ \AA}$ , Ref. 22).

length has been the subject of debate.<sup>21,22</sup> We have adapted the value  $d_{\text{Si-H}} = 1.41 \text{ \AA}$  found by Estreicher.<sup>22</sup> Furthermore, the convergence of the LDOS as a function of the cluster size has been established.<sup>4</sup>

The atomic positions and bond lengths were taken to agree with the known average values.<sup>19,20</sup> The exact atomic positions of the silicon atoms could be obtained from energy minimizing calculations or diffraction experiments, but instead small changes in atomic positions and bond lengths were found to produce negligible changes in the obtained results.

In Fig. 2 we depict the pLDOS and LDOS calculations of  $\text{SiO}_x$  ( $x = 0, 0.5, 1, 1.5, 2$ ). In Table I we compare our calculated results (LDOS) with experimental data of Refs. 23 and 24.

Studying the formation of  $\text{SiO}_2$  (of the order of a few monolayers) with ultraviolet photoelectron spectroscopy (UPS), Ibach and Rowe<sup>23</sup> and Ludeke and Koma,<sup>24</sup> resolved peaks at  $-18.4$ ,  $-15.1$ ,  $-11.9$ , and  $-8.3 \text{ eV}$  below the vacuum level. On the other hand, for the fully oxi-

dized silicon surface, features at  $-20.4$ ,  $-17.1$ , and  $-13.2 \text{ eV}$  were resolved suggesting an entirely different binding structure.

Except for the high-binding-energy features, our calculated peaks resemble those obtained by UPS<sup>23,24</sup> and by calculations of Ciraci *et al.*<sup>25</sup> and Ching.<sup>26</sup> Very localized Si-3s levels (bonding energy  $> -20 \text{ eV}$ ) are also reported by Stanekiewicz<sup>27</sup> and could be interpreted as molecularlike energy levels due to the breakdown of the degeneration of the crystalline electronic bulk structure.

In Fig. 3 we show the calculated  $dA(E)/dE$  spectra of all possible chemical species involved in the silicon-oxide interface. These spectra have been calculated from the pLDOS presented in Fig. 2, using Eq. (1).

In Fig. 4 we present the results of the  $\text{Si-L}_{2,3}VV$  Auger measurements  $dN(E)/dE$  (not loss corrected) for the initial oxidation stages of two vicinal silicon surfaces ( $100$ ,<sup>28</sup>  $110$ <sup>29</sup>) reported earlier. The initial oxidation behavior of the Si(111) surface<sup>30</sup> is very similar to that of the Si(100) surface and is therefore not shown in Fig. 4.

From Fig. 4 we see that the initial adsorption of molecular oxygen does not influence the Auger spectrum significantly for the three vicinal silicon surfaces. Nevertheless, the chemical reactivity is very different for the Si(100) $2 \times 1$  and Si(111) $7 \times 7$  with respect to the Si(110) $5 \times 1$  reconstructed surface, which is clearly shown by the different exposure doses in the caption of Fig. 4. This is in agreement with Hollinger and Himpsel<sup>31</sup> and Aspnes and Theeten.<sup>32</sup> They found that the surface orientation does not play an important role in the structure of the interface, resulting in the same atomic electronic distribution. Kunjunny and Ferry (Ref. 15 and references therein) reported that  $L_{2,3}VV$  peaks of the Si(100, 111, 110) surfaces could be quite similar. This conclusion might be premature due to the lack of resolution in the measured loss distorted Auger spectrum.

Close inspection of the spectra in Figs. 4(a) and 4(b) show subtle differences in its shape. Therefore, we believe that the suggestion that the initial adsorption process, exhibiting roughly the same features in the  $\text{Si-L}_{2,3}VV$  Auger spectrum, needs a more detailed analysis. We tried to enhance the resolution of the Auger spectra by a more ade-

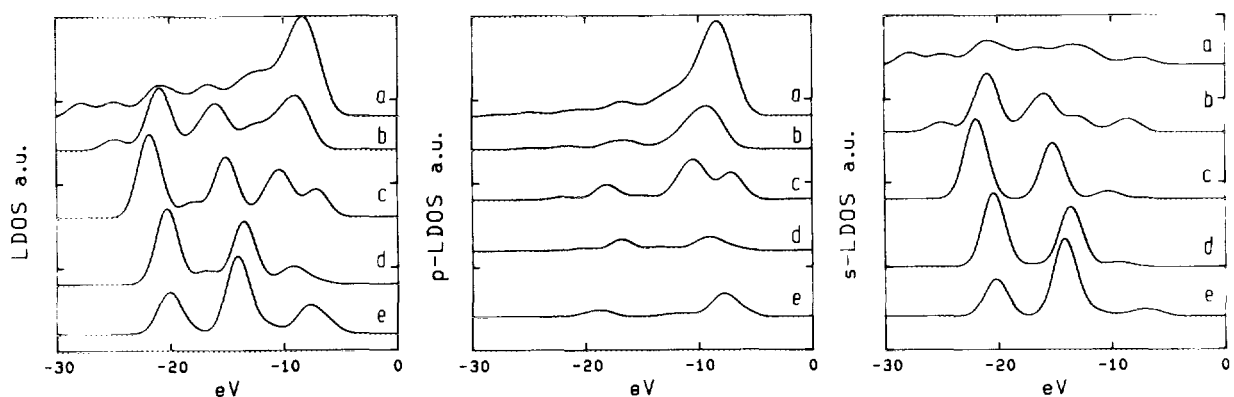


FIG. 2. The partial and the complete LDOS of  $\text{SiO}_x$ : (a)  $x = 0$ , (b)  $x = \frac{1}{2}$ , (c)  $x = 1$ , (d)  $x = \frac{3}{2}$ , and (e)  $x = 2$ . The peak positions are listed in Table I. The vacuum level is taken as zero energy.

TABLE I. Peak positions of the LDOS of  $\text{SiO}_x$ .

$x =$	Peak position in eV (vacuum = 0 eV)					
0	-8.4	-12.6	-16.6	-20.4	-24.6	-28.2
0.5	-9.1	-12.2	-16.0	-21.0	-24.9	...
1	-7.2	-10.5	-15.2	-17.9	-21.9	...
1.5	-9.2	-13.5	-16.8	-20.3	...	...
2	-7.7	-14.1	...	-20.1	...	...
$x = 1$						
UPS (Refs. 23, 24)	-8.3	-11.9	-15.1	-18.4	...	...
$x = 2$						
UPS (Refs. 23, 24)	...	-13.2	-17.1	-20.4	...	...

quate signal processing. We want to present the first results of this scheme for the oxidation of the silicon(100) surface (a few monolayers) to illustrate its potential power (Fig. 5, Table II). The main objective is to illustrate the potential of this scheme of analyzing  $L_{2,3}VV$  Auger spectra. Detailed discussion of the peaks resolved in this scheme for the several oxidation stages of the three low-Miller-index surfaces of silicon will be published in forthcoming publications.

In Fig. 4 we can resolve three distinct peaks at 62, 70, and 83 eV for all the three faces, which can be related to oxygen chemisorption.<sup>28-30</sup>

The peak at 83 eV is the most sensitive Auger transition upon oxygen chemisorption and has been assigned to Si-O bond formation on the first-layer Si atoms.<sup>28</sup> The magnitude of this oxygen induced peak was found to be proportional to the number of disappeared dangling bond surface states.<sup>28</sup> Comparing the experimental obtained peak at 83 eV with the features in the calculated spectra of  $\sim 83$  eV we are able to characterize this transition as a composition of  $pp$  and  $sp$

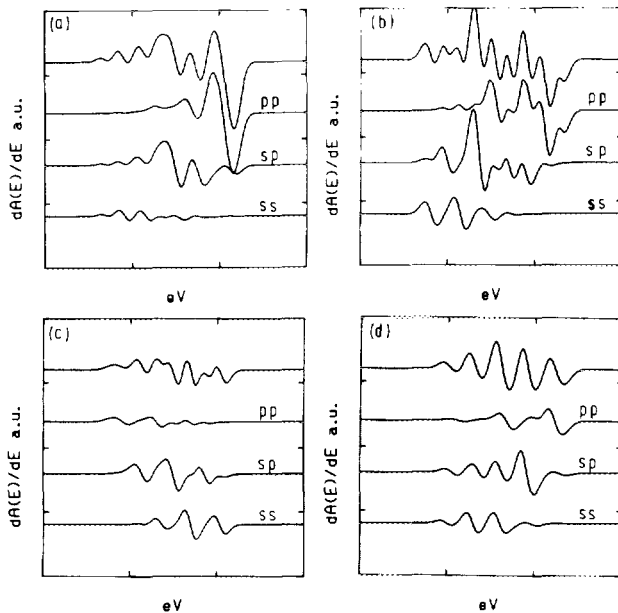


FIG. 3. The calculated  $dA(E)/dE$  spectrum of  $\text{SiO}_x$ : (a)  $x = 0.5$ , (b)  $x = 1$ , (c)  $x = 1.5$ , and (d)  $x = 2$ . The top curve is the sum of the  $ss$ ,  $sp$ , and  $pp$  contributions. The width of the energy axis is 60 eV and the peak positions are listed in Table II.

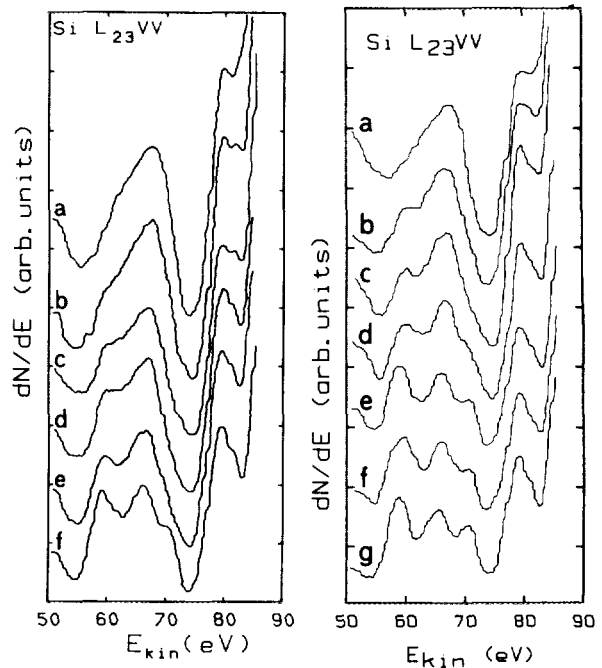


FIG. 4. (Left)  $\text{Si-L}_{2,3}VV$  Auger spectrum for five chemisorption stages of oxygen on silicon: (a) the clean  $\text{Si}(100)2 \times 1$  surface. The surface exposed to  $\text{O}_2$ : (b) 2 L, (c) 4 L, (d) 8 L, (e) 12 L, and (f) 85 L.  $\text{Si-L}_{2,3}VV$  Auger spectrum for five chemisorption stages of oxygen of the clean  $\text{Si}(111)7 \times 7$  surface are identical with that of  $\text{Si}(100)2 \times 1$  surface. (Right)  $\text{Si-L}_{2,3}VV$  Auger spectrum for six chemisorption stages of oxygen on silicon: (a) the clean  $\text{Si}(100)5 \times 1$  surface. The surface exposed to  $\text{O}_2$ : (b) 13 L, (c) 170 L, (d) 1000 L, (e)  $2.7 \times 10^4$  L, (f)  $7.0 \times 10^4$  L, and (g)  $1.0 \times 10^5$  L. (1 L =  $1.0 \times 10^{-6}$  Torr s).

transitions. When Auger holes are positioned on the peaks in the LDOS spectrum (Fig. 3) we can relate the peaks in Table I to these  $ss$ ,  $sp$ , and  $pp$  Auger transitions. Applying the first-order approximation for the kinetic energy of the Auger electrons:

$$E_{\text{kin}} = E_{L_{2,3}} - E_{v1} - E_{v2} - E_{\phi}, \quad (2)$$

where  $E_{L_{2,3}} - E_{\phi}$  is approximated by 100 eV and  $E_{v1}$  and  $E_{v2}$  are related to the peak positions in the LDOS spectra.  $E_{\phi}$  is the energy loss related to the work function. Utilizing this argument we observe that the 83-eV transition in the  $\text{SiO}_{1/2,3/2}$  units is, predominantly  $pp$ -like, constituted of valence electrons of  $p$ -type of approximately  $-9$  eV. In the  $\text{SiO}_{1,2}$  units the  $sp$  transition is more dominant ( $\sim -7$  eV  $p$ -like and  $\sim -13$  eV  $s$ -like valence electrons). The  $pp$  transition intensity decreases at the full oxidation stage ( $\text{SiO}_2$ ). Reference 31 observed also at an early oxidation state features at  $\sim 82$  eV. The character of our calculated Auger transitions for not fully oxidized silicon at  $\sim 82.5$  eV, which are composed of  $p$ -type electrons situated at the top of the valence band is consistent with the experimental results of Keim *et al.*<sup>28-30</sup> and supports the assignment of this peak to Si-O bond formation in the first layer.

The Auger transition at  $\sim 70$  eV is composed of  $ss$  and  $sp$  type and has been attributed to bulklike oxide.<sup>28-30,33</sup> In the calculated  $\text{SiO}_{1/2}$  spectrum this peak is almost absent and is increasing upon further oxidation. Furthermore, this peak is shifted towards lower kinetic energy level of  $\sim 69$  eV at more

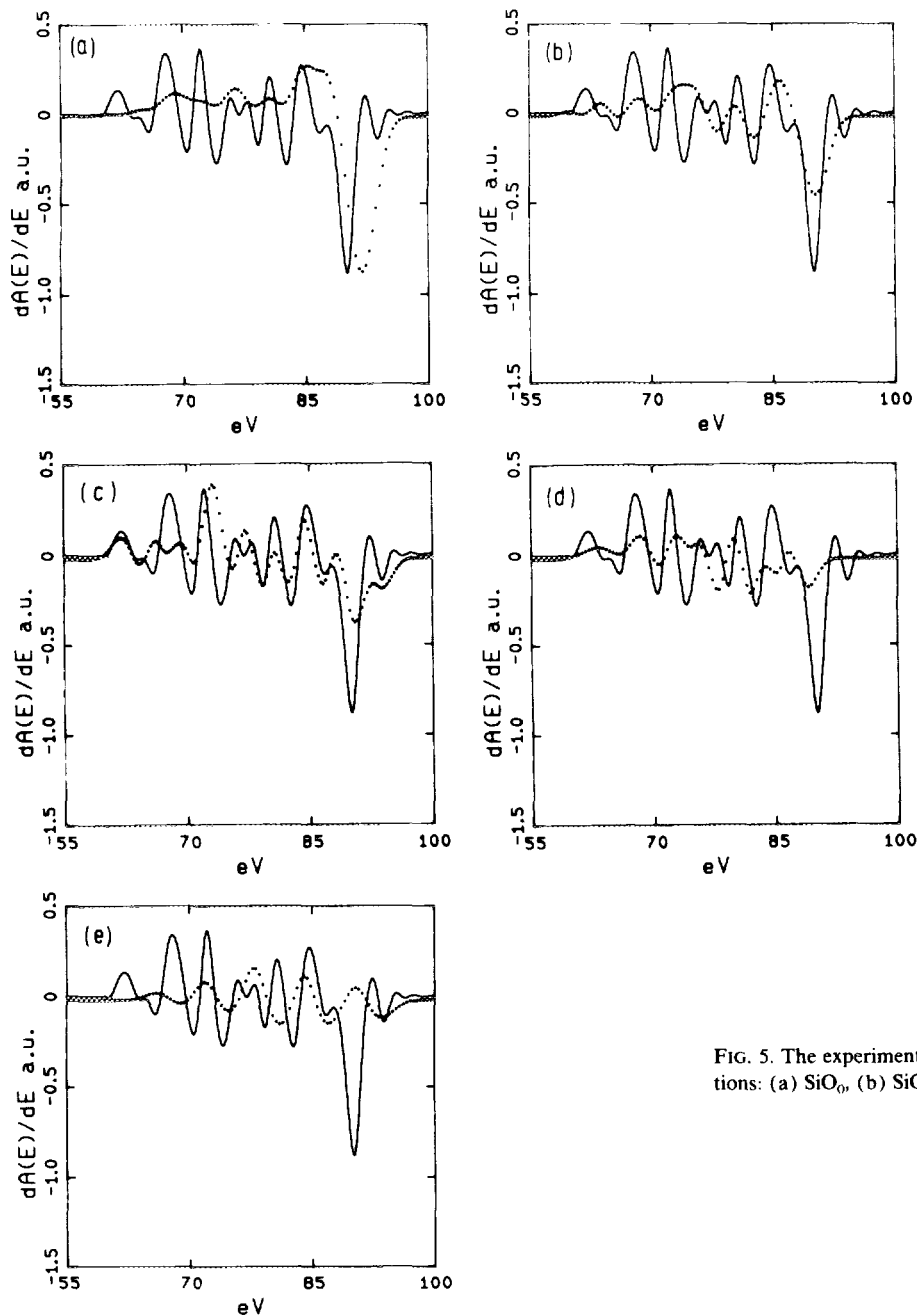


FIG. 5. The experimental  $dA(E)/dE$  spectrum is compared with calculations: (a)  $\text{SiO}_0$ , (b)  $\text{SiO}_{1/2}$ , (c)  $\text{SiO}_1$ , (d)  $\text{SiO}_{3/2}$ , and (e)  $\text{SiO}_2$ .

advanced oxidation stages, which also observed experimentally by others.<sup>28,31</sup> However, the 70-eV transition also emerges when atomic oxygen is bridge bonded to dimers or backbonds ( $\text{SiO}_1$  and  $\text{SiO}_{3/2}$ ) and can therefore not entirely be attributed to bulklike oxide ( $\text{SiO}_2$ ).

The peak at  $\sim 62$  eV, which has been assigned to unstable silica,<sup>36,37</sup> is also predominantly an *ss*-like Auger transition ( $\sim -20$  eV in the LDOS in Fig. 2). However, this peak emerges in all oxidation stages and even the LDOS spectrum of the clean silicon surface (Fig. 2). This peak in the LDOS remains approximately constant for  $\text{SiO}_x$  ( $x = 1, \frac{3}{2}, 2$ ). The existence of this peak for  $\text{SiO}_2$  suggests that it cannot be attributed entirely to unstable silica. Furthermore, this peak can be composed of many different types of Auger transitions, which could be the cause for the shift of this peak in

the calculated spectra, for the several oxidation stages.

The main peak of the  $\text{Si-L}_{2,3}VV$  Auger transition at 91.8 eV is shifted to  $\sim 90.4$  eV. The shift of  $\sim 1.4$  eV in the Auger spectrum is also observed in the  $dA(E)/dE$  calculation [Table II: 91.9 eV ( $\text{SiO}_0$ )–90.5 eV ( $\text{SiO}_1$ )]. Furthermore, the shift of the main peak is even larger for  $\text{SiO}_2$ . The shifts in the calculated spectra are completely caused by changes of the energy levels of the valence electrons upon oxygen adsorption. No correction for possible core-level shifts upon variation of the chemical environment, which we believe is neglectable, is made.

The transitions, 90.4, 83, 70, and 62 eV, of the spectra in Fig. 4 are resolved by the calculated results of  $\text{SiO}_1$ , 90.5, 82.3, 70.8, and 64.2 (Table II). The additional peaks in this calculated spectrum are obscured, in the  $dN(E)/dE$  Auger

TABLE II. Peak positions of the  $dA(E)/dE$  of  $\text{SiO}_x$  ( $x = 0, 0.5, \dots, 2$ ).

$x =$	Peak position in eV (calculated)									
	0	...	91.9	86.5	82.3	79.0	74.0	71.3	65.6	...
0.5	...	90.4	...	82.7	78.1	...	70.6	66.0	...	61.4
1	93.8	90.5	86.5	82.3	79.2	75.5	70.8	67.5	64.2	...
1.5	...	89.1	85.0	82.0	78.0	74.6	70.7	65.5	...	...
2	93.6	...	87.0	81.1	...	74.9	68.9	...	...	...
	Peak position in eV (measured)									
	$\text{SiO}_x$ (Ref. 31) <sup>a</sup>	...	...	84.5	82.0	78.0	75.0	69.0	66.5	64.0
$\text{SiO}_2$ (Ref. 31) <sup>a</sup>	...	...	...	...	78.0	...	...	66.0	...	61.5
$\text{SiO}_x$ (Ref. 15) <sup>a</sup>	...	89.0	85.0	83.0	79.0	75.0	71.0	69.0	...	...
$\text{SiO}_2$ (Ref. 32) <sup>a</sup>	...	...	...	...	76.1	73.1	68.4	...	...	61.1
$\text{Si}(100)\text{-O}_2$ <sup>b</sup>	93.8	90.3	86.8	82.7	79.2	74.1	70.5	65.8	...	60.1
Fig. 5										
$\text{SiO}_x$	...	90.4	...	83.0	...	...	70.0	...	...	62.0
Fig. 4										

<sup>a</sup> These spectra are presented in the  $A(E)$  mode. The peak positions in the derivative mode is defined in respect to the maximum negative-going peak, which induces a small difference with peaks in the  $A(E)$  mode.

<sup>b</sup> Our result of the signal processing.

spectra, by the strong plasmon transition at 74 eV,<sup>35</sup> which overlaps with the real spectrum and by the broadening of the main peak by inelastic losses.<sup>6</sup>

Upon comparing the calculated results with the loss corrected measured result most of the additional structures predicted (Table II, Fig. 5) are resolved experimentally. In Table II also loss deconvoluted results of other workers are included, which are in a close agreement with our obtained results. In Fig. 5 we compare the measured  $dA/dE$  with the calculated oxidation stages. We observe that all four stages resemble part of the measured spectrum, which supports the results of Hollinger and Himpsel,<sup>33,38</sup> who suggested a multiple-bonding configuration. They found, approximately, a ratio of  $\text{SiO}_x$  ( $x < 2$ ) of 33% each.

The  $p$ -type character of the LDOS of the clean Si surface changing upon adsorption to a  $s$ -type LDOS makes it impossible to resemble completely the whole measured spectrum (Fig. 5, solid line) with a calculated one (Fig. 5, dashed lines). In the  $\text{SiO}_{1/2}$  (mainly  $p$  type) we observe a quite good agreement at the high kinetic energy part ( $p$  type) of the spectrum and reverse at  $\text{SiO}_{3/2}$  (mainly  $s$  type). The best overall agreement is obtained for  $\text{SiO}_1$ . No significant  $\text{SiO}_2$  components were found. The intensity of the calculated spectra are not to scale with respect to each other, this, for convenience in comparing its structure. The relative intensity is decreasing on further chemisorption.

In conclusion, the described scheme of analyzing  $\text{SI-L}_{2,3}$   $VV$  Auger data in the derivative mode, corrected for all kinds of loss mechanisms, in combination with quantum chemical calculations (MINDO/3) proves to be a powerful tool in analyzing Auger line shapes in terms of local density of states of the valence electrons. Furthermore, new peaks could be resolved, which were obscured in the  $dN(E)/dE$  mode. Subtle changes in the Auger line shape  $A(E)$  due to chemisorption of oxygen could be detected and character-

ized. The method of calculation used is flexible upon modeling local chemisorption processes and reveals valence electron distributions positioned in real space.

Also, supporting evidence is given that at least three intermediate oxidation stages are present in the monolayer range.

The presented scheme of analyzing the chemisorption stages by measuring the  $CVV$  Auger transitions gives promising new opportunities for gaining chemical information from solid surfaces and makes a new step in the future intention to apply Auger electron spectroscopy (AES) as a source of information about the surface chemical bond, electron correlation effects, or local density of states, in addition to mere element detection.

<sup>1</sup>F. J. Himpsel, Appl. Phys. A **38**, 205 (1985).

<sup>2</sup>H. Ibach, H. D. Bruchmann, and H. Wagner, Appl. Phys. A **29**, 113 (1982).

<sup>3</sup>D. E. Ramaker, J. S. Murday, N. H. Turner, C. Moore, M. G. Lagally, and J. E. Houston, Phys. Rev. B **19**, 5375 (1979).

<sup>4</sup>A. G. B. M. Sasse, H. Wormeester, M. A. van der Hoef, and A. van Silfhout, Phys. Rev. B (submitted); A. G. B. M. Sasse, M. A. van der Hoef, and A. van Silfhout, in Proceedings of the 19th ICPS, Warchaw, 1988 (in press).

<sup>5</sup>P. H. Holloway, Adv. Electron. Electron Phys. **54**, 241 (1980).

<sup>6</sup>H. Wormeester, A. G. B. M. Sasse, and A. van Silfhout, Comp. Phys. Comm. **52**, (1989); A. G. B. M. Sasse, H. Wormeester and A. van Silfhout, Surf. Interface Anal. **14**, (1989).

<sup>7</sup>P. J. Feibelman, E. J. McGuire, and K. C. Pandey, Phys. Rev. B **5**, 2202 (1977); P. J. Feibelman and E. J. McGuire, *ibid.* **17**, 690 (1978).

<sup>8</sup>D. E. Ramaker, *Chemistry and Physics of Solid Surfaces. IV*. Springer Series in Chemical Physics, Vol. 20, edited by R. Vanselow and R. Howe (Springer, Berlin, 1982), p. 19; D. E. Ramaker, F. L. Hutson, N. H. Turner, and W. N. Mei, Phys. Rev. B **33**, 2574 (1986).

<sup>9</sup>D. R. Jennison, Phys. Rev. B **18**, 6865 (1978).

<sup>10</sup>D. R. Jennison, Phys. Rev. Lett. **40**, 807 (1978).

<sup>11</sup>D. E. Ramaker, Phys. Rev. B **25**, 7341 (1982).

<sup>12</sup>D. E. Ramaker, Phys. Rev. B **21**, 4608 (1980).

<sup>13</sup>J. A. D. Matthew and Y. Komninos, Surf. Sci. **53**, 716 (1975).

- <sup>14</sup>R. Weissman, K. Muller, Surf. Sci. Rept. **1**, 251 (1981).  
<sup>15</sup>T. Kunjunny and D. K. Ferry, Phys. Rev. B **24**, 4593 (1981).  
<sup>16</sup>M. J. S. Dewar, J. Phys. Chem. **89**, 2145 (1985).  
<sup>17</sup>M. J. S. Dewar, R. C. Binham, and D. H. Lo, J. Am. Chem. Soc. **97**, 1285 (1975).  
<sup>18</sup>P. Bischof, J. Am. Chem. Soc. **98**, 6844 (1976).  
<sup>19</sup>D. J. Chadi, Phys. Rev. Lett. **43**, 43 (1979).  
<sup>20</sup>W. S. Verwoerd, Surf. Sci. **99**, 581 (1980).  
<sup>21</sup>A. A. Bonapaste, C. Battistoni, A. Lapiccirilla, N. Tomassini, S. L. Altmann, and K. W. Lodge, Phys. Rev. B **37**, 3058 (1988).  
<sup>22</sup>S. Estreicher, Phys. Rev. B **37**, 858 (1988).  
<sup>23</sup>H. Ibach and J. E. Rowe, Phys. Rev. B **10**, 710 (1974).  
<sup>24</sup>R. Ludeke and A. Koma, Phys. Rev. Lett. **34**, 1170 (1975).  
<sup>25</sup>S. Ciraci, S. Ellialtioglu, and S. Erkoc, Phys. Rev. B **26**, 5716 (1982).  
<sup>26</sup>W. Y. Ching, Phys. Rev. B **26**, 6633 (1982).  
<sup>27</sup>B. Stankiewicz, Phys. Status Solidi B **134**, 691 (1980).  
<sup>28</sup>E. G. Keim, Surf. Sci. **148**, L641 (1984); E. G. Keim, L. Wolterbeek, and A. van Silfhout, *ibid.* **180**, 565 (1987).  
<sup>29</sup>E. G. Keim and A. van Silfhout, Surf. Sci. **187**, L557 (1987); E. G. Keim, A. van Silfhout, and L. Wolterbeek, J. Vac. Sci. Technol. A **6**, 57 (1988).  
<sup>30</sup>E. G. Keim and A. van Silfhout, Surf. Sci. **152/153**, 1096 (1985); E. G. Keim, A. van Silfhout, and L. Wolterbeek, J. Vac. Sci. Technol. A **5**, 1019 (1987).  
<sup>31</sup>M. L. Knotek and J. E. Houston, J. Vac. Sci. Technol. B **1**, 899 (1983).  
<sup>32</sup>P. Morgen, J. H. Onsgaard, and S. Tongaard, Appl. Phys. Lett. **50**, 874 (1979).  
<sup>33</sup>G. Hollinger and F. J. Himpsel, Appl. Phys. Lett. **44**, 93 (1984).  
<sup>34</sup>D. E. Aspnes and J. B. Theeten, J. Electrochem. Soc. **127**, 1359 (1980).  
<sup>35</sup>A. G. B. M. Sasse, D. G. Lakerveld, and A. van Silfhout, Surf. Sci. **195**, L167 (1988).  
<sup>36</sup>C. Fiori, Phys. Rev. Lett. **52**, 2077 (1984).  
<sup>37</sup>C. Fiori and R. A. B. Devine, Phys. Rev. Lett. **52**, 2081 (1984).  
<sup>38</sup>G. Hollinger and F. J. Himpsel, Phys. Rev. B **28**, 3651 (1983).